

Extensions of the orthogonal beamforming to identify multiple multipole sources

Xingjian PAN¹; Weikang JIANG¹;

¹ Shanghai Jiao Tong University, China

ABSTRACT

Identification of sources with complex directivities is attracting great attentions in aeroacoustic measurements these years. A multipole orthogonal beamforming algorithm was proposed to identify multipoles with arbitrarily oriented axes with no prior knowledge about source types. Independent sources were separated by the eigenvalue decomposition of the cross spectral matrix of signals measured by microphone arrays. The influence of source directivities on source imaging was eliminated by normalizing and squaring the eigenvectors. The delay-and-sum procedure was performed on each modified eigenvector to localize sound sources. The proposed algorithm was verified by simulations and experimental trials using a combination of a loudspeaker and an Aeolian tone dipole source. The accuracy of estimated source positions is improved and the resolution of the proposed algorithm is comparable to that of deconvolution approaches.

Keywords: Aeroacoustic measurements, Beamforming, Multipole sources

1. INTRODUCTION

Beamforming techniques have been widely applied to identify aeroacoustic noise sources such as airframe noise, airfoil noise and broadband fan noise(1-3). Most delay-and-sum beamforming algorithms and deconvolution approaches use source models of monopoles and produce source imaging by compensating for the phase delay between assumed sources and microphones(4). However, most aeroacoustic noise sources have non-uniform directivities and are often analogous to multipole sources. For example, sources arising from flow-body interactions have a two-lobed directivity pattern and are analogous to dipole sources. Beamforming methods based on the monopole model may lead to incorrect estimations of positions of aeroacoustic sources with complex directivities.

Studies on beamforming methods for multipole sources have been carried out over recent years. Schmidt *et al.* presented the multipole-detection algorithm based on the conventional beamforming(5). It replaced the steering vector with a 'steering matrix' whose columns correspond to sources of different types. Pre-defined source types and orthogonal radiation patterns were required. A beamforming method for directional sources was proposed by Bouchard(6), in which the source model based on the spherical harmonic expansion is used and a set of 'sub-beamformers' is defined to response to different spatial modes of a source. The prior knowledge of source positions was required. The $L1$ generalized inverse beamforming method was introduced by Suzuki(7). It obtained eigenmodes through the eigen decomposition of the cross spectral matrix of array signals and reconstructed the source distribution using generalized inverse techniques. The method was restricted to pre-defined monopoles and multipoles whose orientations were on the plane parallel to the array.

The objective of this study is to develop a beamforming algorithm that is capable of estimating the positions and strengths of multipole sources without knowing their types or orientations. The basic idea of the orthogonal beamforming is used that individual eigenvalues and eigenvectors of the signal subspace are linked to sources or source mechanisms(8). This idea is further extended that these eigenvectors also contain information of source directivities. Normalization and square operations on the eigenvectors can remove the influence of source directivities on source imaging.

The outline of the paper is as follows. After the introduction, the multipole orthogonal beamforming is presented in Section 2. Simulation results are discussed in Section 3. The proposed

¹ xj_pan@sjtu.edu.cn

method is verified by experimental trials using a loudspeaker and an Aeolian tone dipole setup in Section 4. Conclusions are drawn in Section 5.

2. THE MULTIPOLE ORTHOGONAL BEAMFORMING

2.1 Modeling the sound field

An array with N_{mic} microphones is used for measurements. In the presence of a single multipole source, the sound pressure p measured by the i -th microphone at \mathbf{x}_i is

$$p(\mathbf{x}_i) = a(\mathbf{x}_i, \mathbf{x}_0, \mathbf{x}_s)q(\mathbf{x}_s), \quad (1)$$

where q is the sound pressure at a reference position \mathbf{x}_0 radiated from that source. Generally, the center of the microphone array is chosen as the reference position on the premise that q does not approach zero. For a free sound field, the transfer function a is related to the source directivity and the source position and is given by

$$a(\mathbf{x}_i, \mathbf{x}_0, \mathbf{x}_s) = \frac{r_0}{r_i} \frac{F_i}{F_0} e^{-jk(r_i - r_0)}, \quad (2)$$

where $r_i = |\mathbf{x}_s - \mathbf{x}_i|$ indicates the distance between the source position and the microphone position. $r_0 = |\mathbf{x}_s - \mathbf{x}_0|$ represents the distance between the source position and the reference position. F_i and F_0 are the directivity functions at the i -th microphone and the reference position. The directivity function is related to the source type and the space angle.

For N_s multipole sources with various directivities, the vector of sound pressures measured by the microphone array is given by

$$\mathbf{p} = \mathbf{A}\mathbf{q} + \mathbf{n}, \quad (3)$$

where the N_{mic} -by- N_s matrix \mathbf{A} is the transfer matrix whose elements are transfer functions described by Eq. (2). The noise signal \mathbf{n} is assumed to be uncorrelated to source signals.

The cross spectral matrix of array signals can be written as

$$\mathbf{C} = E\{\mathbf{p}\mathbf{p}^H\}, \quad (4)$$

where $E\{\}$ represents the expectation operator and H denotes the conjugate transpose. Since the cross spectral matrix is non-negative definite and Hermitian, it can be decomposed as

$$\mathbf{C} = \mathbf{U}\mathbf{\Lambda}\mathbf{U}^H, \quad (5)$$

where \mathbf{U} is a unitary matrix whose columns are eigenvectors of the cross spectral matrix \mathbf{C} . $\mathbf{\Lambda}$ is a diagonal matrix whose diagonal elements are eigenvalues λ_i of the cross spectral matrix.

2.2 Descriptions of the algorithm

It is assumed that the multiple sources to be identified are mutually incoherent and spatially orthogonal(9), and background noise is uncorrelated to source signals. Therefore, the eigenvectors of the cross spectral matrix of array signals can be divided into two parts, including the signal subspace spanned by the first N_s eigenvectors and the noise subspace spanned by the rest. According to the orthogonal beamforming, eigenvectors of the signal subspace are linked to sound sources or source mechanisms. Information of directivities and positions of sources is contained in the eigenvectors, and the eigenvalues contain information of source strengths.

To eliminate the influence of source directivities on source imaging, elements of the unitary matrix \mathbf{U} are all normalized and squared as

$$v_{ij} = \left(\frac{u_{ij}}{|u_{ij}|} \right)^2, \quad (6)$$

where u_{ij} is the j -th element of the i -th eigenvector of the cross spectral matrix. A modified matrix composed of elements v_{ij} is generated as $\mathbf{V} = [\mathbf{v}_1, \mathbf{v}_2 \dots \mathbf{v}_{N_{\text{mic}}}]$, where v_{ij} is the (i, j) th element. The normalization procedure aims to remove amplitudes of directivity functions contained in sound pressures. Because the directivity functions may be negative and increase the pressure phase by π , the normalized elements are squared to compensate for the phase change. As a result, the signal subspace is transformed into a subspace exclusive of source directivities. The first N_s modified eigenvectors are then used to localize the multiple sources.

Using each eigenvalue λ_i and the corresponding modified eigenvector \mathbf{v}_i , a matrix $\mathbf{D}_i = \lambda_i \mathbf{v}_i \mathbf{v}_i^H$ can be calculated. The matrix is used to generate a beamforming map as

$$B_i(\xi_j) = \mathbf{h}(\xi_j)^H \mathbf{D}_i \mathbf{h}(\xi_j). \quad (7)$$

where ξ_j is the j -th grid point on the scanning plane. \mathbf{h} is the steering vector whose i -th component satisfies

$$h_i = \frac{1}{N_m} e^{-2jk(r_i - r_0)}. \quad (8)$$

Compared with the steering vector of the conventional beamforming, the phase of each element of the modified steering vector is twice larger because the square procedure described by Eq. (6) enlarges the pressure phase. Source strengths estimated by Eq. (7) are much smaller than real ones because the normalization procedure in Eq. (6) changes the amplitudes of sound pressures. This underestimation can be corrected by compensating for the amplitudes as

$$B_i(\xi_j) = \frac{\mathbf{u}_i^H \mathbf{u}_i}{N_m} \mathbf{h}(\xi_j)^H \mathbf{D}_i \mathbf{h}(\xi_j). \quad (9)$$

The source map generated by Eq. (9) corresponds to a single multipole source. The highest peak in the map is estimated as the source position. For a better resolution, the map is replaced by a ‘clean beam’ as

$$Q_i(\xi_j) = B_{i_max} 10^{-\alpha \|\xi_j - \xi_{max}\|^2}. \quad (10)$$

The beamforming output of all the multipole sources is given by

$$Q(\xi_j) = \sum_{i=1}^{N_s} Q_i(\xi_j). \quad (11)$$

The number of sources N_s can be assessed by using the criterion of ‘entropic L-curve’ (10) or other criteria based on the estimated eigenvalues.

3. NUMERICAL SIMULATIONS

In this section, two simulation cases were conducted to analyze the properties of the multipole orthogonal beamforming. The first simulation case was to identify four quadrupoles with different orientations. It was designed to evaluate the performance of the algorithm on localizing multipoles of the same type. The second one was to identify two quadrupoles and two dipoles with different orientations. Its purpose was to investigate the capabilities of identifying multipoles of different types. Beamforming results were compared with some existing algorithms including the conventional beamforming (CB)(4), CLEAN-SC(11) and the orthogonal beamforming (OB)(8).

3.1 Generation of simulation data

In the first simulation case, four quadrupoles at the frequency of 4000 Hz were placed on the y - z plane as shown in Figure 1(a). Generated sources in the second case were at the same frequency and set on the same positions as shown in Figure 1(b). An array of 56 microphones was installed in a distance of 1m away from the source plane with the array center located on the x -axis. Relative positions of the microphones and sources were shown in Figure 2. A $0.6\text{m} \times 0.6\text{m}$ scanning plane was set on the y - z plane with 0.02m spacing and 1681 grid points.

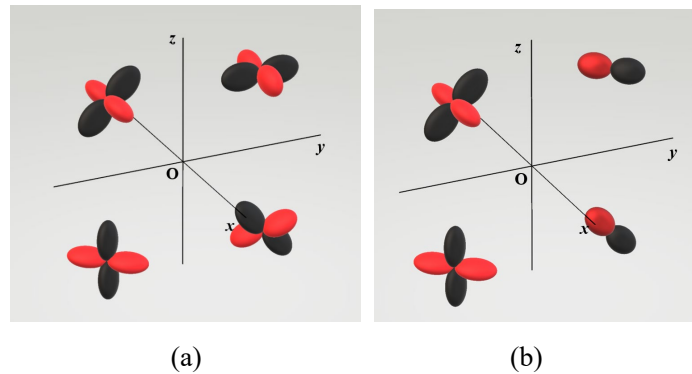


Figure 1 – The directivities of multipole sources in simulations. Case 1 (a) contained four quadrupoles and

Case 2 (b) contained two dipoles and two quadrupoles.

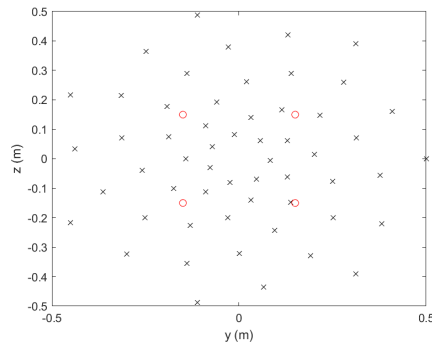
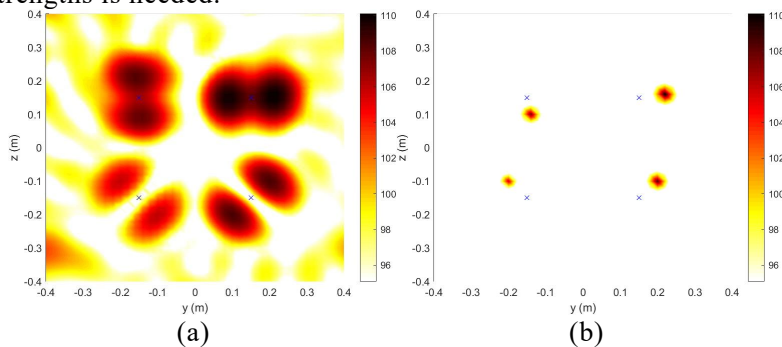


Figure 2 – The schematic representation of the simulation setup: the \times symbols denote the positions of microphones and the red circles denote the positions of sources. The microphone array was set parallelly 1m away from the source plane.

3.2 Results and discussions

Source maps of the first case produced by using four beamforming algorithms are shown in Figure 3. Beamforming patterns of quadrupoles generated by CB are all separated into two side lobes with small outputs in real source positions. Positions of sources estimated by CLEAN-SC and OB deviate from the correct ones considerably although their beamforming patterns are focused. The inaccurate estimation of source positions is influenced by source directivities. The directivity functions of quadrupoles act as weighting parameters in the beamforming procedure. The steering vectors of beamforming algorithms based on the monopole model only consider the influence of measurement distances and cannot compensate for the directivity functions. Consequently, beamforming outputs are not only determined by the phase delay between assumed sources and microphones but also influenced by the amplitude variance caused by source directivities. It leads to a distorted source map. The multipole orthogonal beamforming eliminates the amplitude difference and recovers the source map by normalizing and squaring elements of eigenvectors. A small deviation may be caused by the decomposition procedure.

Source strengths estimated by the four beamforming algorithms are nearly the same. However, different from a monopole source, sound pressures radiated from a multipole source are not only related to the source strength and the measurement distance but also the directivity function and the space angle. Microphone arrays placed at different space angles may output different source levels. It impedes the further investigation of the nature of sources. Further research on the estimation of absolute source strengths is needed.



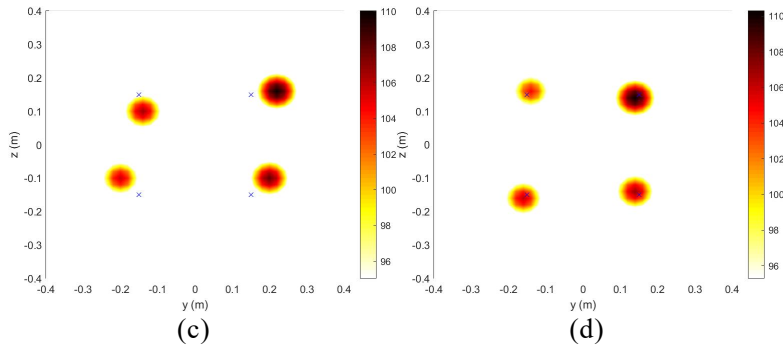


Figure 3 – Source maps of four quadrupoles with different orientations produced by four beamforming algorithms, including (a) CB, (b) CLEAN-SC, (c) OB and (d) the multipole orthogonal beamforming.

Source maps of two dipoles and two quadrupoles in the second case are shown in Figure 4. Similarly, beamforming algorithms based on the monopole model lead to an inaccurate estimation of source positions. The deviation is related to the types and orientations of sources. For dipole sources with their axes closer to the normal of the microphone array, the source positions are estimated more accurately. The proposed multipole orthogonal beamforming can still localize the sources accurately regardless of their types and orientations.

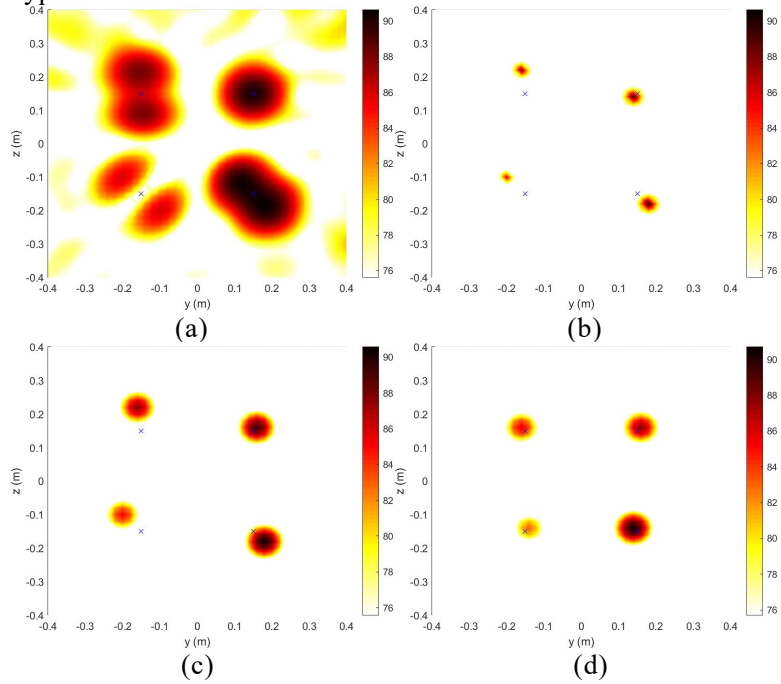


Figure 4 – Source maps of two dipoles and two quadrupoles with different orientations produced by four beamforming algorithms, including (a) CB, (b) CLEAN-SC, (c) OB and (d) the multipole orthogonal beamforming.

4. EXPERIMENTAL VERIFICATION

Experimental trials were conducted to investigate the performance of the multipole orthogonal beamforming in a more practical environment. The experimental setup was shown in Figure 5(a), including a microphone array, a loudspeaker, a 4mm circular cylinder and an air duct. The open jet flow produced by the air duct was around 35 m/s. An Aeolian tone dipole source could be induced by the flow over the circular cylinder. The loudspeaker was set above the cylinder and had a uniform directivity as a monopole source. The microphone array was installed parallel to the flow direction in a distance of 0.5 m.

Two cases were tested when the circular cylinder was parallel and vertical to the ground, as shown in Figure 7 (b) (c). In theory, the oriented axis of the Aeolian tone dipole source is

perpendicular to the plane composed of the flow direction and the cylinder. Therefore, the dipole axis was respectively parallel and vertical to the array in Case 1 and 2. It is well established that the Strouhal number $St = fD/U$ is approximately equal to 0.21 for the flow around a circular cylinder, and the dipole frequency equals the vortex shedding frequency when the Reynold number Re is more than 5000. For this experimental setup, the flow velocity was around 35 m/s, and the corresponding source frequency was 1835 Hz. Given that the flow velocity was unsteady, a 1/3 octave band centered at 2000 Hz was analyzed. Four beamforming algorithms were applied and compared, including CB, CLEAN-SC, OB and the proposed multiple orthogonal beamforming.

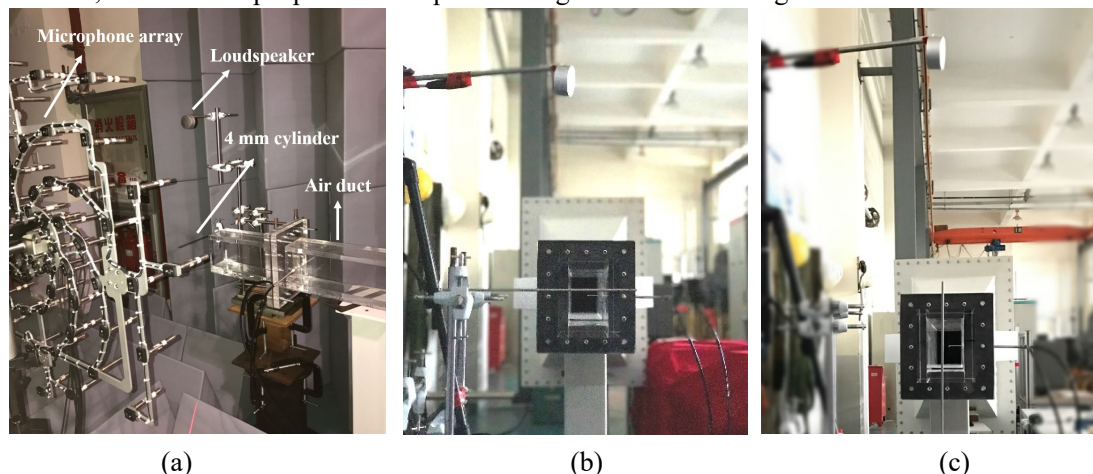
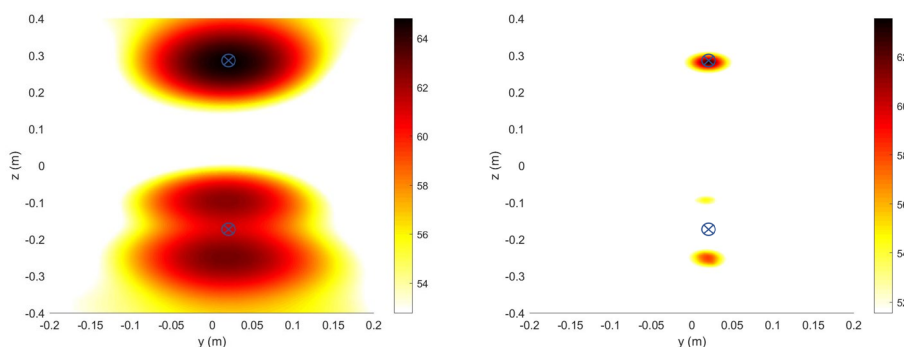


Figure 5 – The experimental setup to produce an Aeolian tone dipole source and a monopole source. (a) shows the trial facilities. (b) shows the setup for Case 1, which produces a dipole whose axis parallel to the array. (c) shows the setup for Case 2, which produces a dipole whose axis vertical to the array.

Sound maps of the first case are shown in Figure 6. For the dipole source whose axis parallel to the array, CB, CLEAN-SC and OB all produce distorted beamforming patterns. The beamforming pattern of the dipole source is separated into two side lobes with a small output in the real source position. It is easy to misinterpret this beamforming pattern as two individual sources. The multipole orthogonal beamforming localizes the dipole source accurately and the resolution is comparable to that of the CLEAN-SC algorithm. Source levels estimated by OB and multipole OB are 2 dB lower than the outputs of CB and CLEAN-SC. It is because side lobes contributed from the background noise have been removed by the eigenvalue decomposition. Source maps of the second experimental case are presented in Figure 7. All four beamforming algorithms estimate the source positions accurately. In this case, the dipole axis is vertical to the microphone array and the dipole source looks like a monopole source from the array direction. Directivity functions of the dipole source over the microphone array vary a little and have a negligible influence on source imaging.

In general, the impact of source directivities on source imaging can be eliminated by the normalization and square operation described by Eq. (6). The multipole orthogonal beamforming can localize multiple independent multipole sources regardless of their types and orientations. This algorithm can be applied to identify airframe noise sources or airfoil noise sources in the wind tunnel, which have complex directivities.



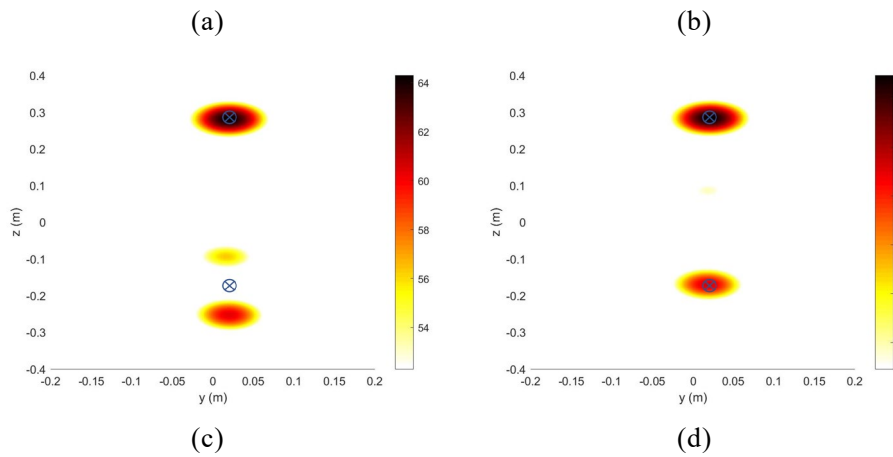


Figure 6 – Source maps of a monopole source and an Aeolian-tone dipole whose axis parallel to the array. Maps are produced by four beamforming algorithms, including (a) CB, (b) CLEAN-SC, (c) OB and (d) the multipole orthogonal beamforming.

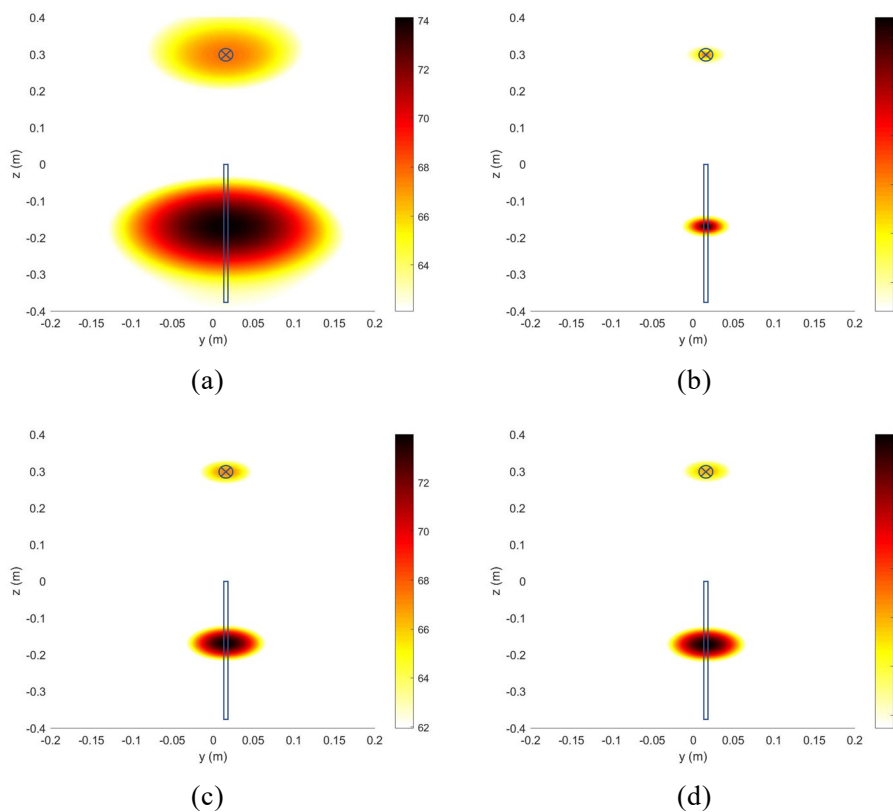


Figure 7 – Source maps of a monopole source and an Aeolian-tone dipole whose axis vertical to the array. Maps are produced by four beamforming algorithms, including (a) CB, (b) CLEAN-SC, (c) OB and (d) the multipole orthogonal beamforming.

5. CONCLUSIONS

A new beamforming method was developed to identify multiple independent multipole sources regardless of their types or orientations. Compared with beamforming algorithms based on the monopole model, the multipole orthogonal beamforming estimates positions of multipole sources more accurately, especially when the source axis deviates from the normal of the microphone array. Compared with other multipole beamforming algorithms, it needs no prior knowledge of source types, orientations or positions. The resolution of this algorithm is comparable to that of deconvolution approaches with moderate computational effort. Further research can be conducted on the estimation of source types and absolute

source strengths.

ACKNOWLEDGEMENTS

This work was supported by National Natural Science Funds of China (Grant No. 11574212).

REFERENCES

1. Stoker R, Guo Y, Streett C, Burnside N, editors. Airframe Noise Source Locations of a 777 Aircraft in Flight and Comparisons with Past Model-Scale Tests. 9th AIAA/CEAS Aeroacoustics Conference and Exhibit; 2003 2003-05-12. Hilton Head, South Carolina: American Institute of Aeronautics and Astronautics.
2. Porteous R, Prime Z, Doolan CJ, Moreau DJ, Valeau V. Three-dimensional beamforming of dipolar aeroacoustic sources. *J Sound Vib.* 2015;355:117-34.
3. Dougherty RP, Walker BE, Sutliff DL. Locating and Quantifying Broadband Fan Sources using In Duct Microphones. 16th AIAA/CEAS Aeroacoustics Conference 2010 31st AIAA Aeroacoustics Conference. 2010:531-49.
4. Sarradj E. Three-dimensional acoustic source mapping with different beamforming steering vector formulations. *Adv Acoust Vib (USA)*. 2012:12.
5. Schmidt R, Franks R. Multiple source DF signal processing: An experimental system. *IEEE Transactions on Antennas and Propagation*. 1986;34(3):281-90.
6. Bouchard C, Havelock DI, Bouchard M. Beamforming with microphone arrays for directional sources. *J Acoust Soc Am*. 2009;125(4):2098-104.
7. Suzuki T. L1 generalized inverse beam-forming algorithm resolving coherent/incoherent, distributed and multipole sources. *J Sound Vib*. 2011;330(24):5835-51.
8. Sarradj E. A fast signal subspace approach for the determination of absolute levels from phased microphone array measurements. *J Sound Vib*. 2010;329(9):1553-69.
9. Dong B, Antoni J, Pereira A, Kellermann W. Blind separation of incoherent and spatially disjoint sound sources. *J Sound Vib*. 2016;383:414-45.
10. Dong B, Antoni J, Zhang E. Blind separation of sound sources from the principle of least spatial entropy. *J Sound Vib*. 2014;333(9):2643-68.
11. Sijtsma P, editor CLEAN Based on Spatial Source Coherence. 13th AIAA/CEAS Aeroacoustics Conference (28th AIAA Aeroacoustics Conference); 2007 2007-05-21. Rome, Italy: American Institute of Aeronautics and Astronautics.